JEF/DOC-297

Evaluation of neutron cross sections and gamma-ray data for chromium and iron isotopes in the energy range 1.0 - 20.0 MeV.

F.Fabbri, G.Maino, E.Menapace and A.Mengoni

ENEA, CRE "E.Clementel", viale Ercolani 8, Bologna, Italy.

Within the framework of a general study of neutron-induced reactions on structural materials /1/, we have performed a complete evaluation of cross sections and related data, such as emitted-particle spectra, etc., for all stable chromium and iron isotopes in the incident-neutron energy range between 1.0 MeV - when the continuum region begins - and 20.0 MeV. Particular care has been devoted to the calculation of gamma-ray production cross sections and spectra since they represent a basic information for many important applications ranging from radiation shielding analysis to heating estimate in both fission and fusion devices, while reliable experimental data are often lacking above all at higher energies. Moreover, investigation of photon-production mechanisms in neutron-induced reactions deserves some interest from a theoretical point of view too, allowing for more

complete and stringent tests of nuclear-reaction models and related computing codes /2/.

Natural chromium and iron are elements of actual importance as structural materials and components of stainless steel, high-temperature alloys, etc., used - for instance - in fast breeder reactors. Natural chromium is a mixture of four stable isotopes : 50Cr (4.35%), 52Cr (83.79%), 53Cr (9.50%) and 54Cr (2.36%). Natural iron consists of 54Fe (5.80%), 56Fe (91.72%), 57Fe (2.20%) and 58Fe (0.28%). An evaluation of neutron and photon-production cross sections and data up to En = 8.0 MeV is described in ref./3/, while preliminary results of a corresponding evaluation for iron isotopes have been presented at previous JEF meetings and in ref./4/. It is worth noting that these calculations have been extended up to En = 20.0 MeV by including preequilibrium contributions evaluated in the frame of the simple exciton model (see *JEF/DOC 276*).

Finally, the evaluated data have been arranged according to ENDF/B format rules and checked by means of standard ENDF utility codes.

Nuclear models and assumptions.

In the considered energy interval, the reaction mechanisms are dominated by direct and statistical processes, while preequilibrium components are important in the higher energy region and mainly affects emitted-particle spectra; however, also preequilibrium contributions to neutron cross sections in the (n,n'), (n,2n), (n,p) and (n,alpha) channels are not negligible and have been added to the statistical values. Direct - semidirect contributions in the neutron radiative capture are important in the MeV region, where the giant dipole resonance acts as doorway state, but heve been neglected in the present work.

As for direct-reaction components are concerned, we used for Cr isotopes the optical model parameters described in ref./3/, while for Fe nuclides the OM parameters derived by Arthur and Young /5/ have been adopted for neutron channels, with only slight adjustements of geometrical parameters in order to achieve a better agreement with experimental information about strength functions and potential scattering radius. As an example, these quantities evaluated for 56Fe are shown in Table I. Moreover, the proton OM parameters of Becchetti and Greenless /6/ have been used since they resulted to work better than other commonly-adopted sets; for the emitted-alpha channel the Igo-Huizenga OM parameters /7/ have been chosen.

Therefore, the calculated OM transmission coefficients have been introduced in the usual Hauser-Feshbach formalism to obtain compound-nucleus formation cross sections for all the channel reactions open in the considered energy range (En < 20 MeV). Statistical fluctuations have been accounted for in all the reaction channels up to En = 3 MeV.

As far as statistical model calculations are concerned, basic ingredients are giant-resonance parameters and nuclear level densities. The choice of most reliable GR parameters is exhaustively discussed in ref./3/, /4/ and previous *JEF/DOC* reports by our group. In table I, the calculated radiative widths for 56Fe in the KeV region are compared with the experimental data. The radiative-capture cross section at En = 30 KeV is in reasonable agreement with the corrsponding measured value. In fig.1 the low-energy tail of the adopted GDR Lorentzian is compared with empirical data deduced from gamma-ray scattering measurements in the photon energy range between 6 and 11 MeV for 56Fe /8/.

The low-energy level schemes and relevant photon-decay branching ratios for all the nuclei involved in the considered neutron-induced reactions have been deduced from recent literature, mainly represented by *Nuclear Data Sheets*, and supplemented by theoretical estimates when the experimental information is lacking or controversial. The adopted nuclear spectra and electromagnetic transitions will be presented in a forthcoming report, actually in preparation /9/.

The level densities for statistical calculations were fitted - at the lower energy side - to the observed number of resolved levels for both parities and, at higher energies, they are able to reproduce, by means of the adopted parameters, the available experimental data, above all from s- and p-wave neutron resonance spacings at the binding energy. We used a simple closed-form expression of Fermi-gas type, corrected for various effects. In particular, odd-even effects have been taken into account by considering an effective excitation energy scaled by the pairing energy; shell contributions have been corrected according to the prescription of Ignatyuk and coworkers /10/, while parity dependence of the nuclear level density has been included by a phenomenological factor /1/, which reproduces microscopic results obtained within the framework of a Nilsson - BCS approach /11/. The adopted level-density formula is presented and discussed in ref./2/; the relevant parameter values for Ti, V, Cr, Mn and Fe isotopes considered in the present evaluations are shown in Table II.

The statistical model calculations have been then performed by means of a modified version of the PENELOPE chain of codes /12/ and the preequilibrium contributions have been properly added once estimated within the exciton model (without angular momentum conservation) /2/.

The cross section for emission of a particular gamma-ray has then obtained by following the photon-deexcitation cascade occurring after each inelastic process induced by the incoming neutron. Photon decay is accounted for at every

stage of reaction channels, before and after all possible particle emissions both in the preequilibrium and statistical models. The average emitted-photon multiplicities have been found to be of the order of six or less in the MeV region, in satisfactory agreement with recent measurements for both (n + 52Cr) and (n + 56Fe) processes at En = 14 MeV /13/.

Results and conclusions.

In figs.2 and foll. we show some selected results both for neutron cross sections and gamma-ray spectra in comparison with the experimental information - when available - for nuclei considered in the present evaluations. They represent the best reached compromise between the need of computational feasibility, nuclear model reliability and physical significance of the adopted relevant parameters, in order to achieve a satisfactory agreement with the available measurements and reliable predictions outside the regions where experimental information exists.

References.

/1/ G.Maino and E.Menapace, *Radiat. Eff.* **95** (1986) 1135; A.Mengoni, F.Fabbri and G.Maino, *Nuovo Cimento* **A94** (1986) 297.

/2/ F.Fabbri, G.Maino, E.Menapace and A.Mengoni, *JEF/DOC 276.*

/3/ A.Mengoni, F.Fabbri and G.Maino, *ENEA report RT/TIB/85/38*, Rome (1985).

/4/ F.Fabbri, G.Maino, E.Menapace and A.Mengoni, *in Proceed. of Int. Conf. on Nuclear Data for Science and Technology*, Mito (1988).

/5/ E.D.Arthur and P.G.Ycung, *Los Alamos report LA-8626-MS* (1980).

/6/ F.D.Becchetti and G.W.Greenless, *Phys. Rev.* **182** (1969) 1190.

/7/ G.Igo and J.R.Huizenga, *Nucl. Phys.* **29** (1962) 462.

/8/ T.Chapuran, R.Starr, R.Vodhanel and M.K.Brussel, *Phys. Rev.* **C30** (1984) 54.

/9/ F.Fabbri, G.Maino and A.Mengoni, *ENEA report* (in preparation).

/10/ A.V.Ignatyuk et al., *Sov. J. Nucl. Phys.* **21** (1975) 21.

/11/ G.Maino and A.Ventura, *Lett. Nuovo Cim.* **37** (1983) 561.

/12/ F.Fabbri and G.Reffo, *unpublished.*

/13/ P.Oblozinsky, in *IAEA report INDC(NDS)-173/GI*, Vienna (1985), p.62; P.Oblozinsky and S.Hlavac, *IAEA report INDC(CSR)-6/GI*, Vienna (1985), p.17.

TABLE I

^{56}Fe statistical calculations in the KeV region.

$\langle \Gamma_{\gamma o} \rangle$ (meV)

- expt. (BNL) = 900
- calc. (30 KeV) = 570

$\langle \Gamma_{\gamma 1} \rangle$

- expt (BNL) = 300
- calc (30 MeV) = 100

$\sigma_{n\gamma}$ (30 KeV)

- expt (BNL) = 15.1±1.3 mb
- calc = 14 mb

S_o ($\times 10^4$)

- expt (BNL) = 2.6±0.6
- calc (10 KeV) = 3.5
- calc (100 KeV) = 2.7

S_1 ($\times 10^4$)

- expt (BNL) = 0.45±0.05
- calc (10 KeV) = 0.64
- calc (100 KeV) = 0.63

R'

- expt (BNL) = 6.1±0.3 fm
- calc (10 KeV) = 7.6 fm
- calc (100 KeV) = 6.5 fm

Reference

BNL: S.F. Mughabghab, M. Divadeenam and N.E. Holden, Neutron Cross Sections, vol. 1 part A, Academic Press, New York (1981)

TABLE II

Level Density Parameters

Mass region 45 < A < 60

Nucleus	a(*) (MeV-1)	gamma (MeV-1)	alfa (MeV-1)	$\Delta_{\zeta}-\delta$ (MeV)	csig2	sig2(lev)	Ecut (MeV)	
46-Ti	(5.250)	0.054	0.20	-0.6898	0.0139	5.2583		
47-Ti	5.467	0.054	0.20	0.5024	0.0139	7.8409		
48-Ti	5.738	0.054	0.20	-1.2853	0.0139	4.6964		
49-Ti	6.148	0.054	0.20	-0.0944	0.0139	7.2692		
50-Ti	6.217	0.054	0.20	-1.9975	0.0139	5.7917		
51-Ti	6.790	0.054	0.20	-0.5587	0.0139	7.9667		
52-Ti								
49-V	(5.750)	0.054	0.40	0.8403	0.0139	7.0714		
50-V	(5.750)	0.054	0.40	1.4105	0.0139	9.0536		
51-V	6.455	0.054	0.40	-0.5750	0.0139	8.2105		
52-V	5.862	0.054	0.40	1.2657	0.0139	6.5536		
53-V	(6.250)	0.054	0.40	0.2702	0.0139	6.7727		
54-V	(6.500)	0.054	0.40	1.1520	0.0139	6.1250		
49-Cr								
50-Cr	(6.000)	0.054	0.40	-0.9089	0.0139	7.2679		
51-Cr	5.582	0.054	0.22	0.7209	0.0139	8.9375		
52-Cr	(6.250)	0.054	0.40	-1.2161	0.0139	9.0662		
53-Cr	6.387	0.054	0.19	-0.1564	0.0139	8.9800		
54-Cr	5.881	0.054	0.40	-0.9692	0.0139	7.0139		
55-Cr	6.529	0.054	0.19	0.0297	0.0139	6.3261		
53-Mn	(6.250)	0.054	0.40	0.4055	0.0139	9.7581		
54-Mn	(6.250)	0.054	0.40	1.4318	0.0139	8.1250		
55-Mn	(6.500)	0.054	0.40	0.2425	0.0139	6.5192		
56-Mn	6.604	0.054	0.40	1.5288	0.0139	7.1685		
57-Mn	(6.750)	0.054	0.40	0.3875	0.0139	7.5833		
58-Mn	(6.850)	0.054	0.40	1.4444	0.0139	6.1250		
52-Fe								
53-Fe	(6.250)	0.054	0.20	0.4612	0.0139	8.9130	3.470	
54-Fe	(6.250)	0.054	0.40	-1.0519	0.0139	6.6875	3.300	
55-Fe	6.728	0.054	0.20	0.2832	0.0139	8.6750	3.080	
56-Fe	(6.750)	0.054	0.40	-1.0518	0.0139	5.6402	4.520	
57-Fe	6.691	0.054	0.20	0.3700	0.0139	4.6875	2.120	
58-Fe	6.277	0.054	0.20	-0.5542	0.0139	6.8472		
59-Fe	7.114	0.054	0.20	0.1138	0.0139	4.5476		

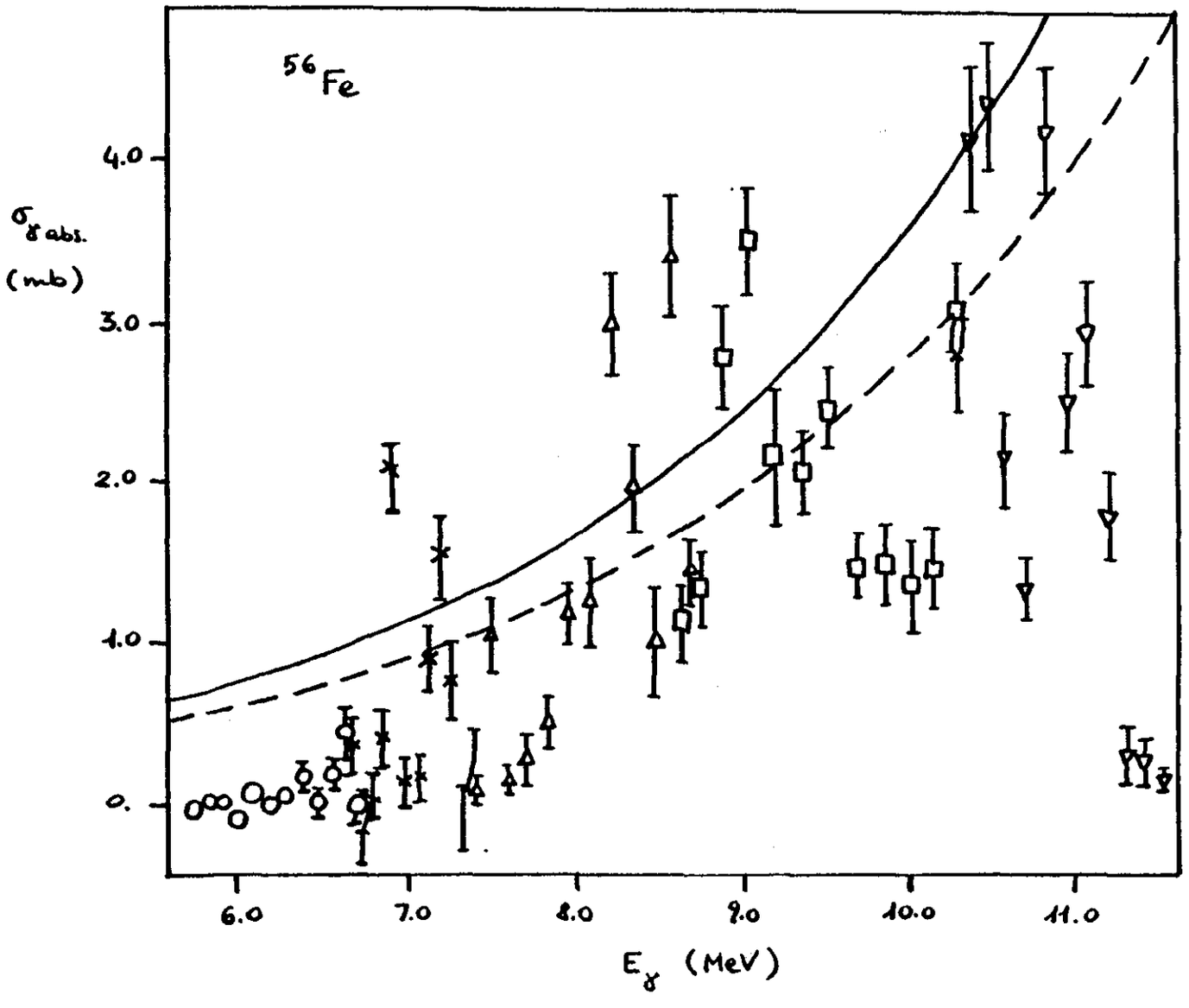

Fig. 1

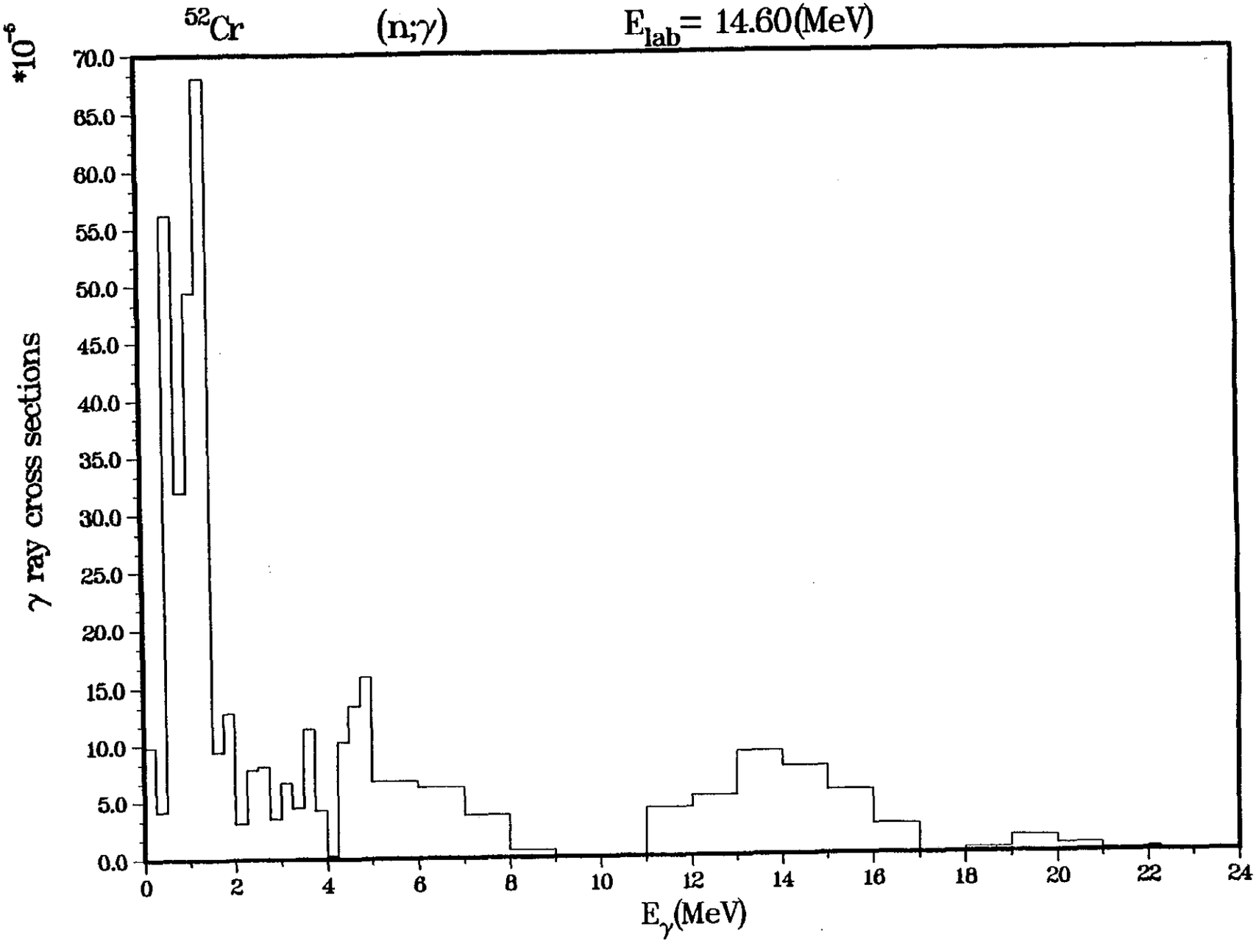

Fig. 2

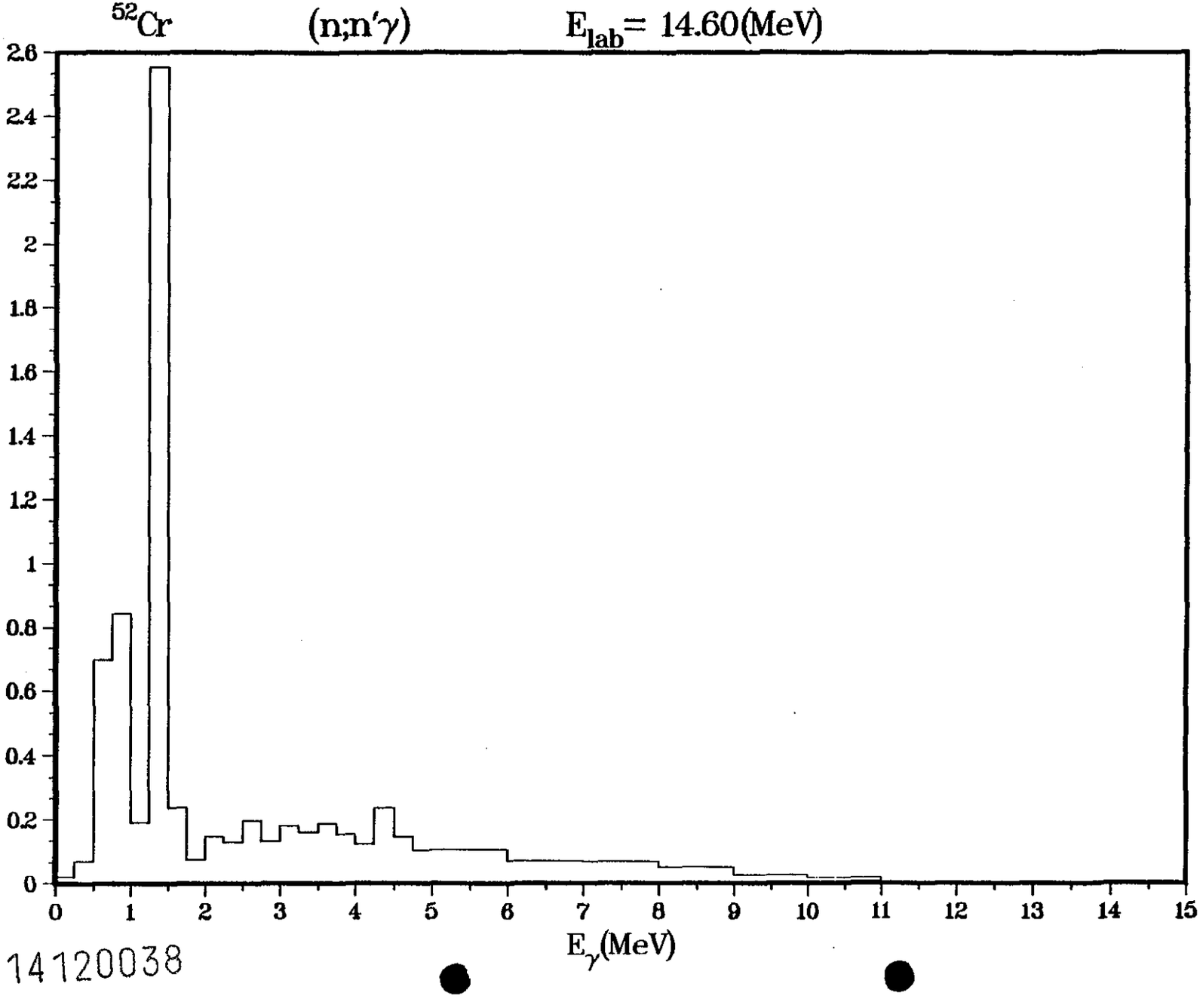

Fig. 3

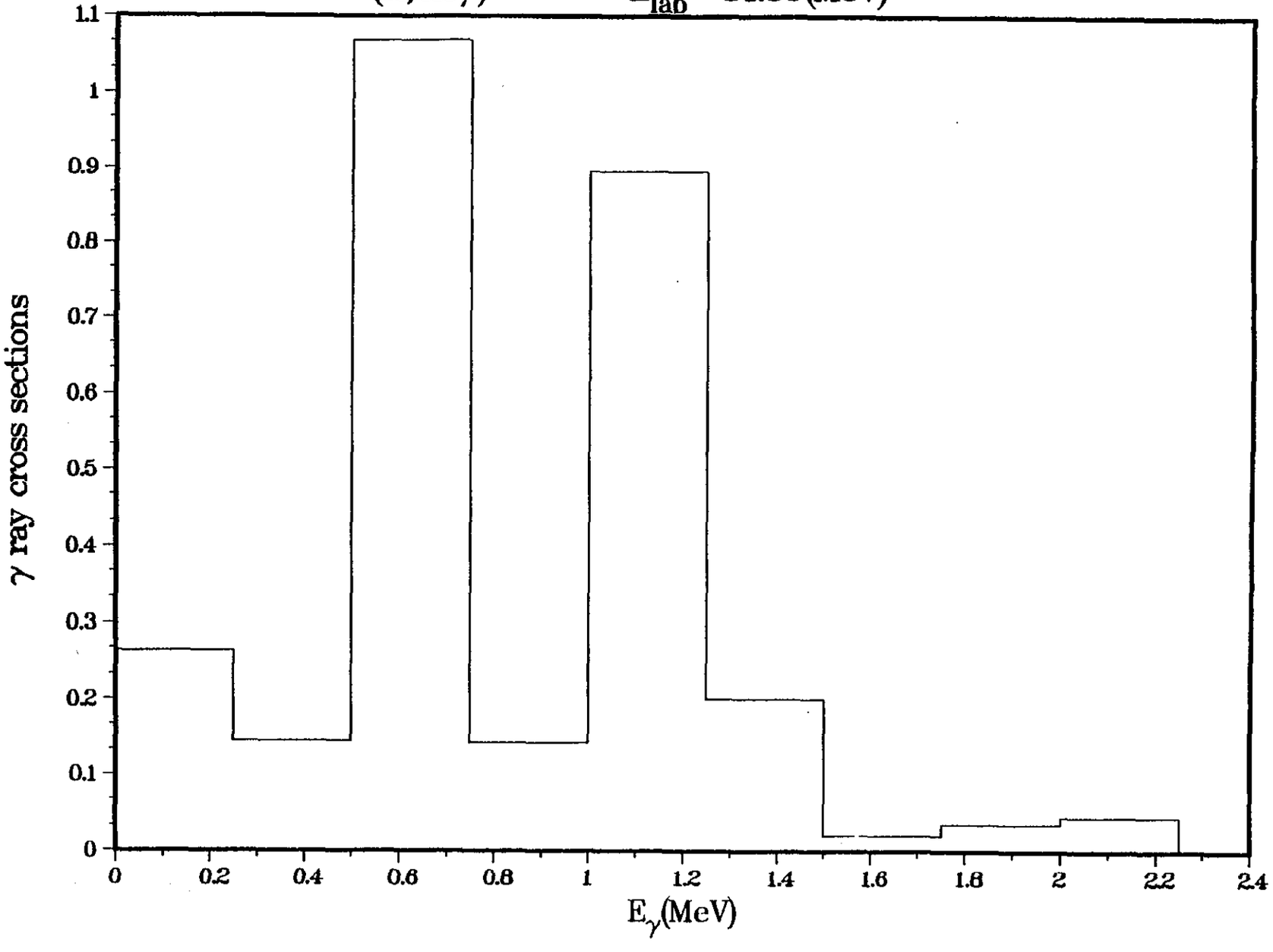

Fig. 4

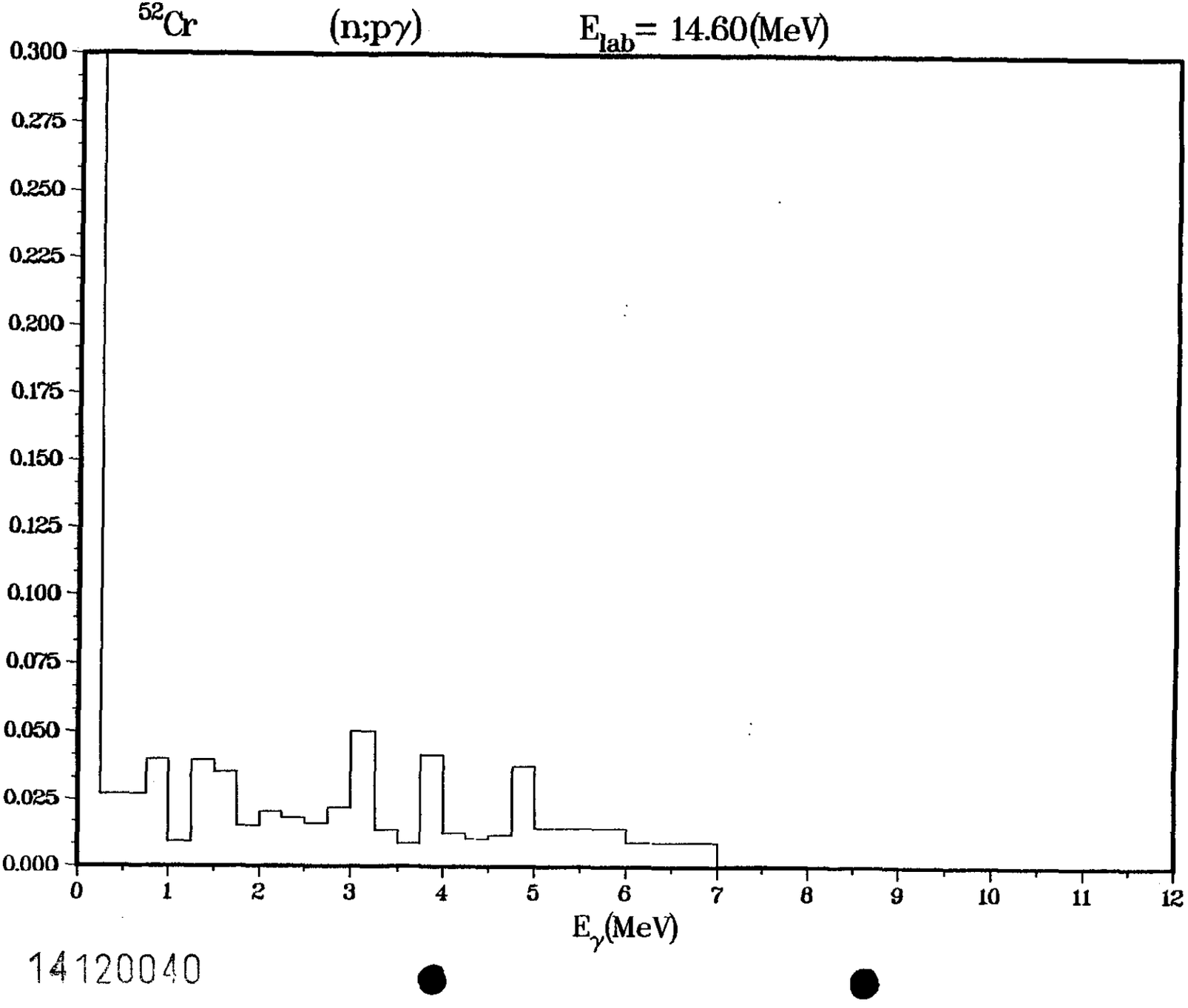

14120040

Fig. 5

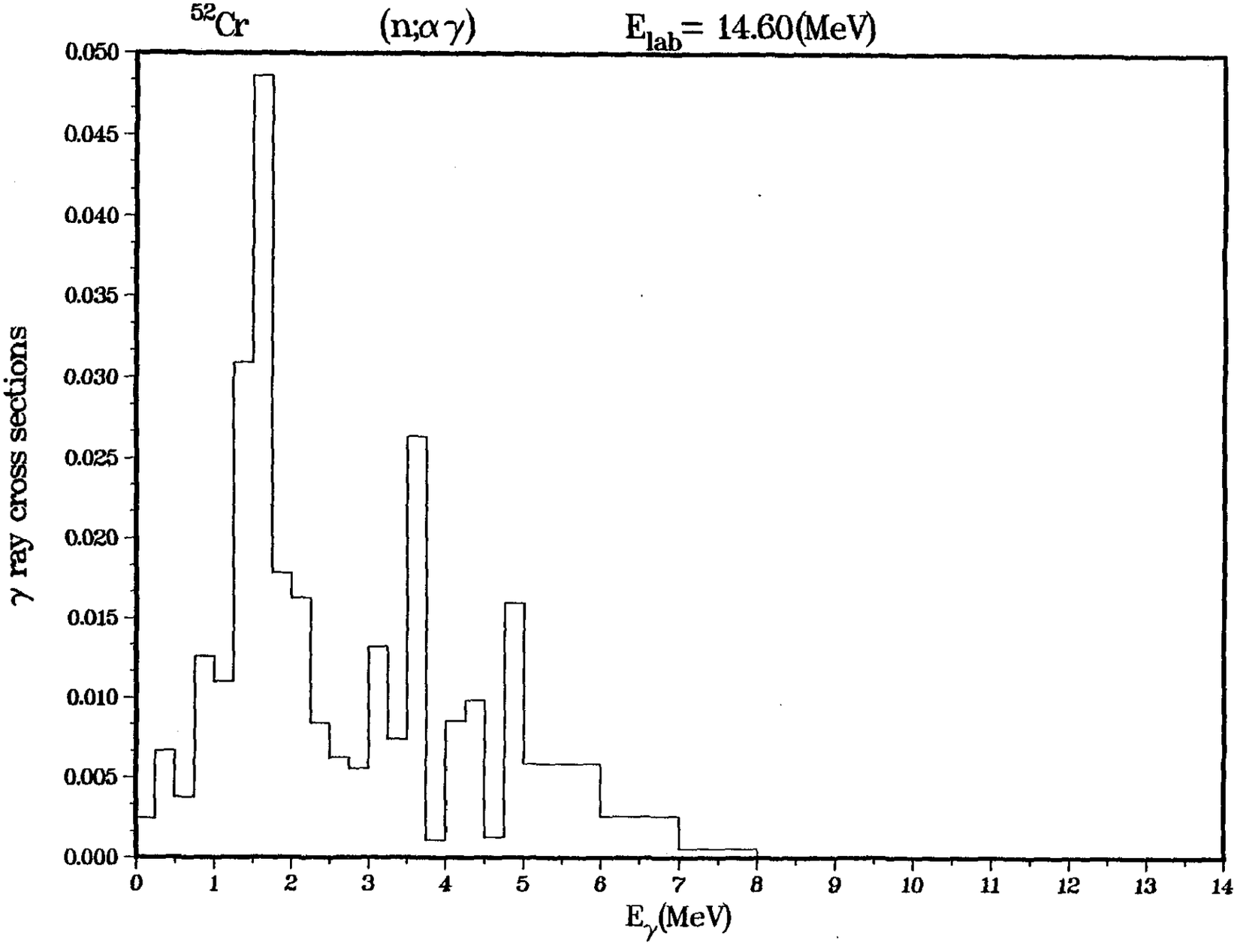

Fig. 6

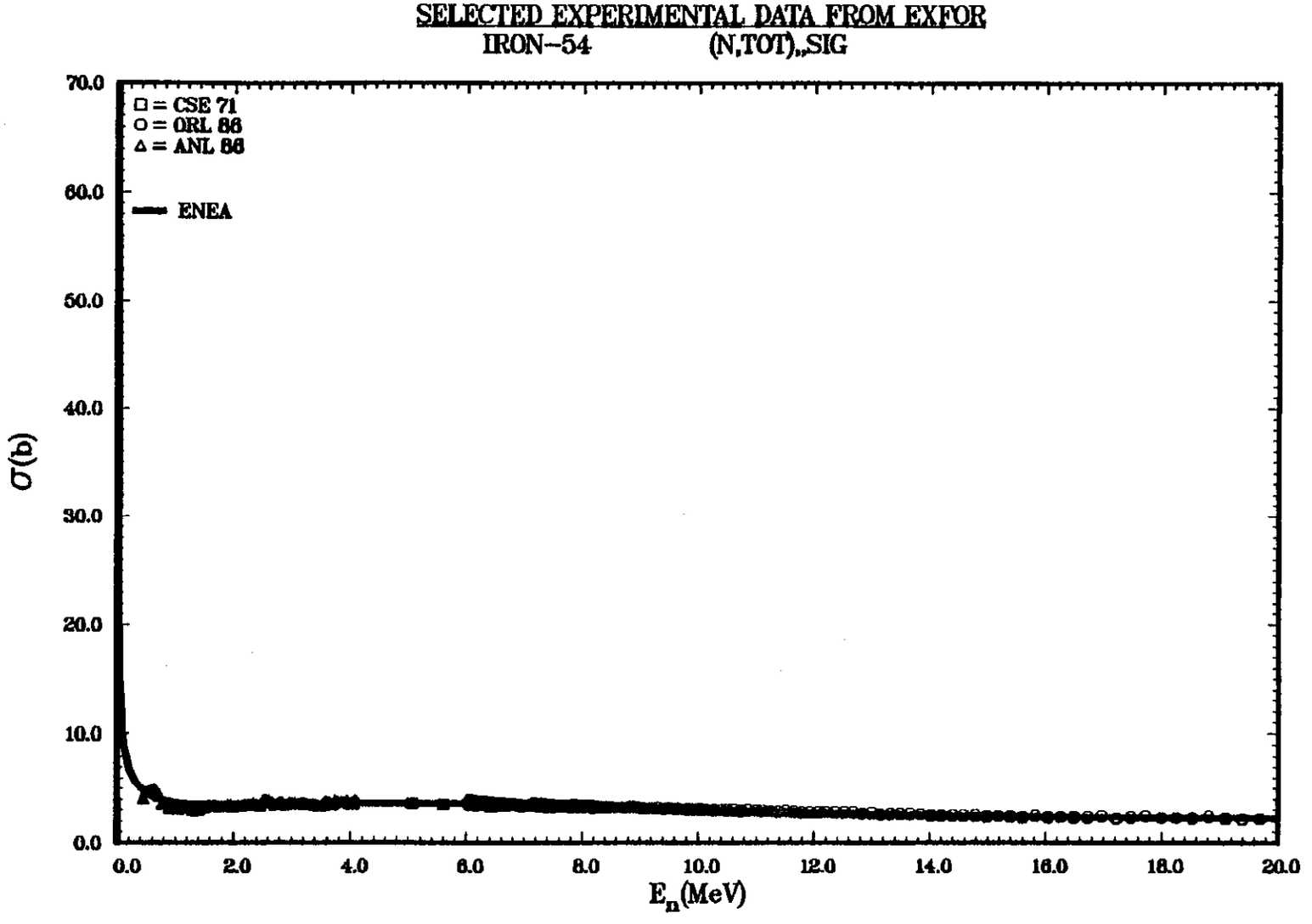

Fig. 7

SELECTED EXPERIMENTAL DATA FROM EXFOR
IRON-54 (N,EI),,SIG

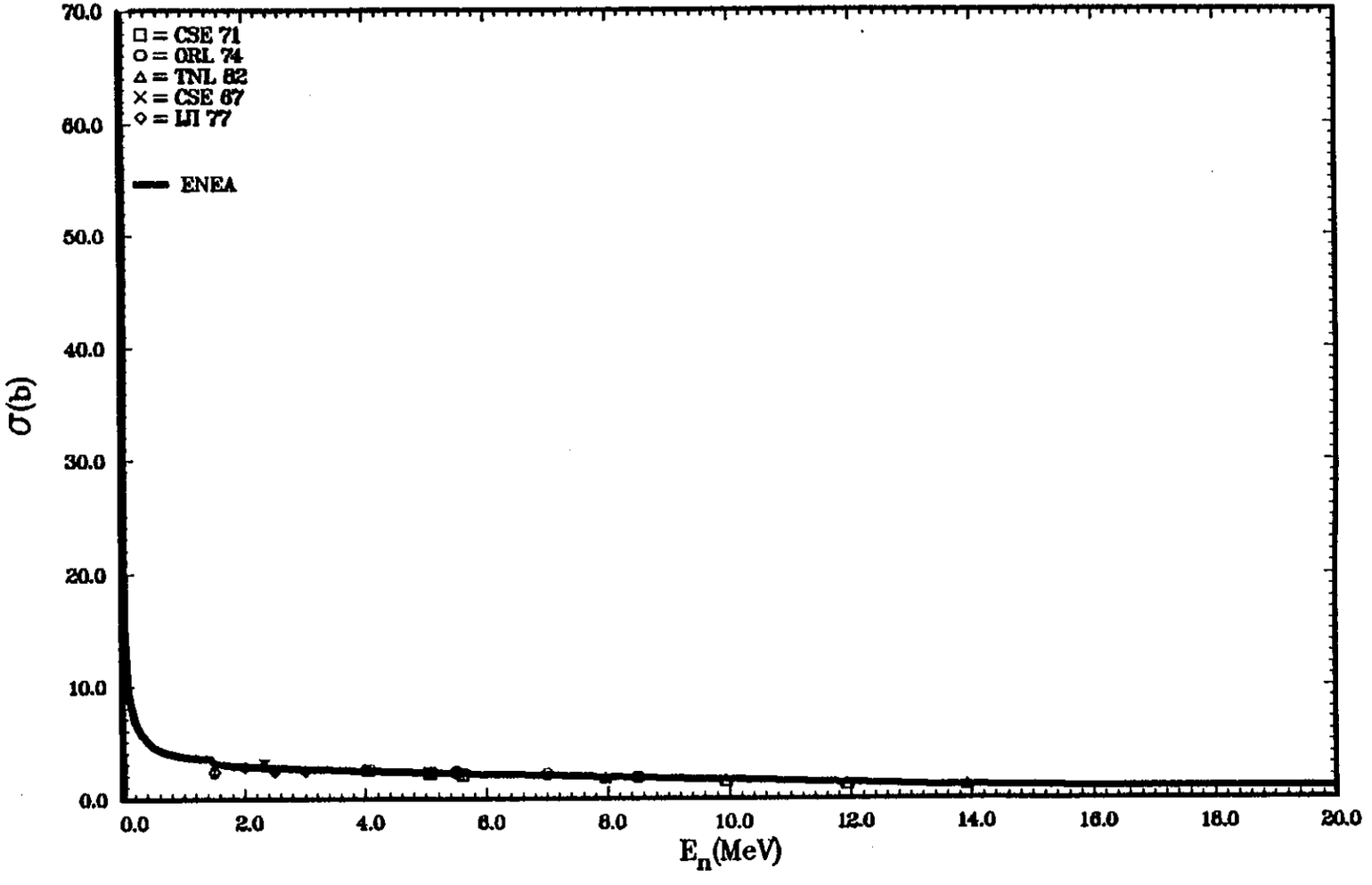

Fig. 8

SELECTED EXPERIMENTAL DATA FROM EXFOR
IRON-54 (N,INL),,SIG

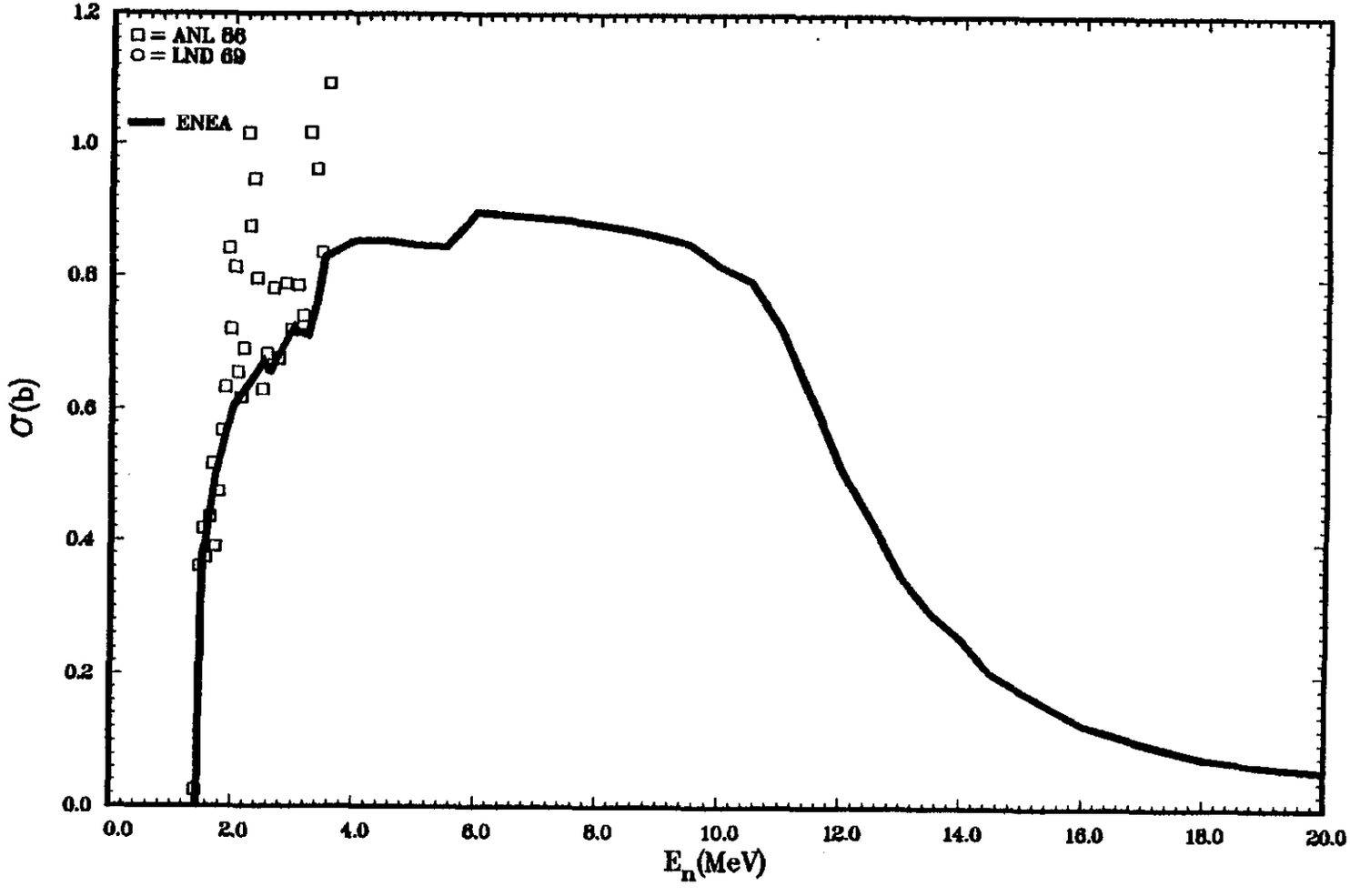

Fig. 9

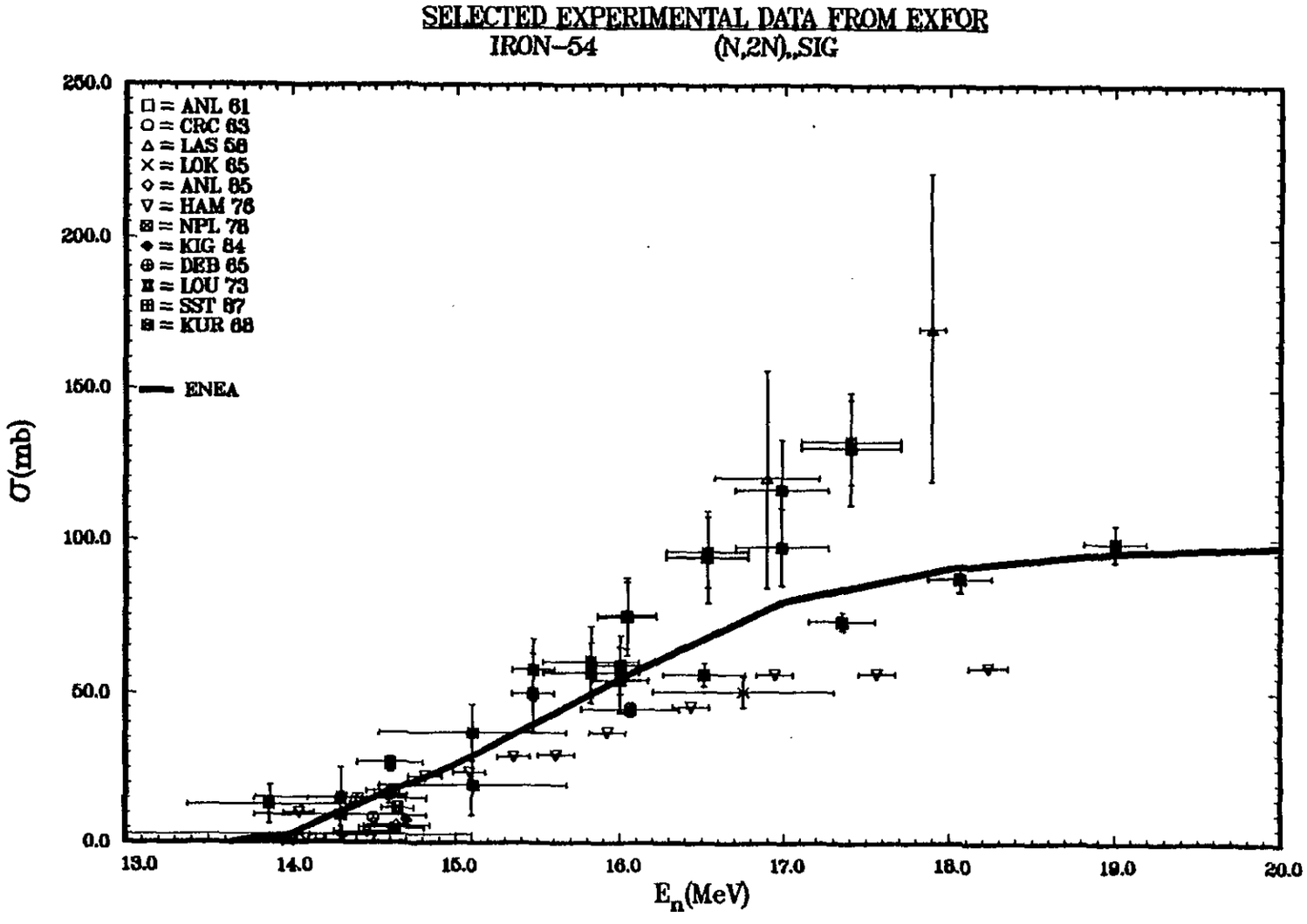

Fig. 10

SELECTED EXPERIMENTAL DATA FROM EXFOR

IRON-54 (N,P),,SIG

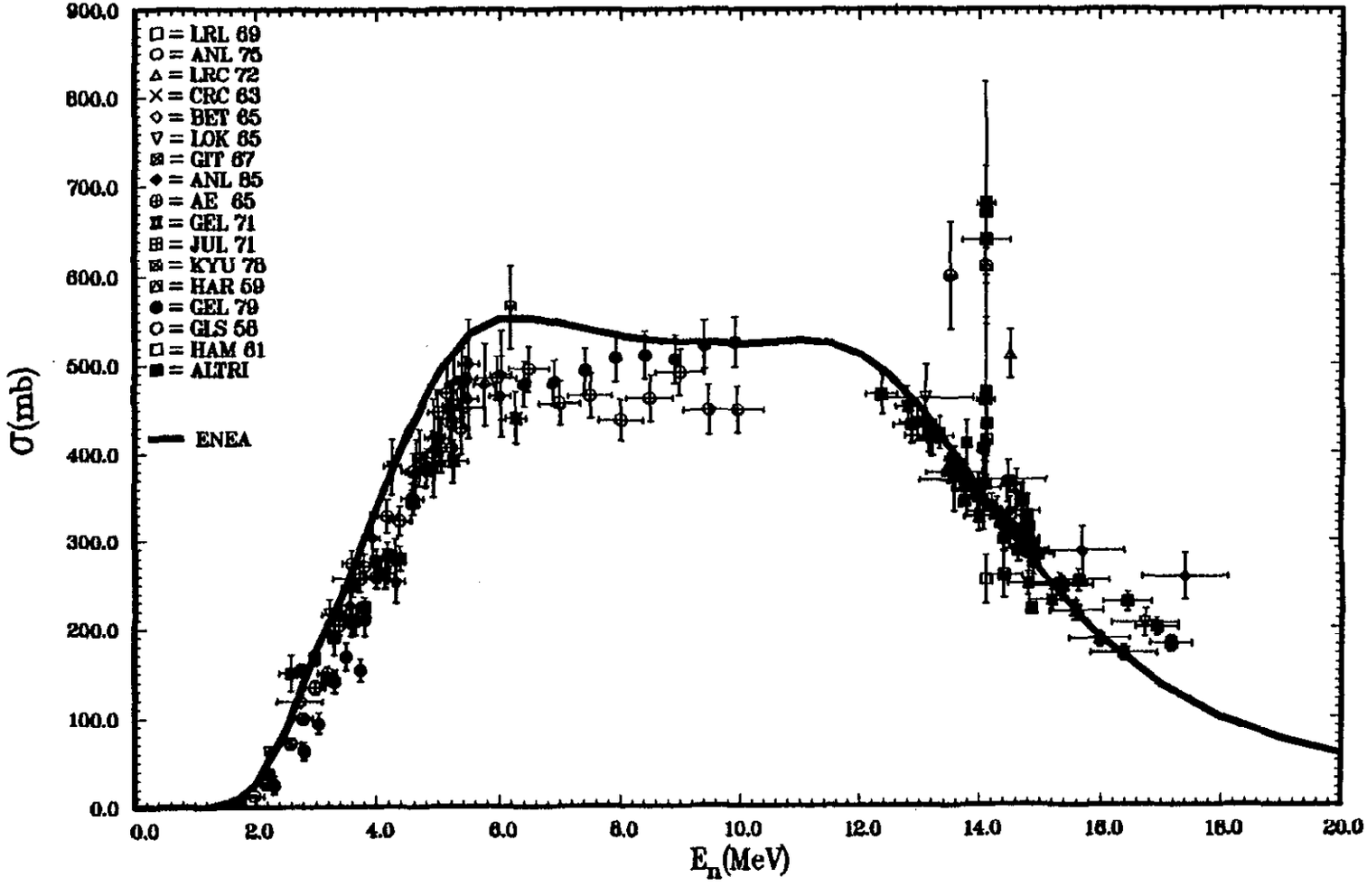

Fig. 11

14120046

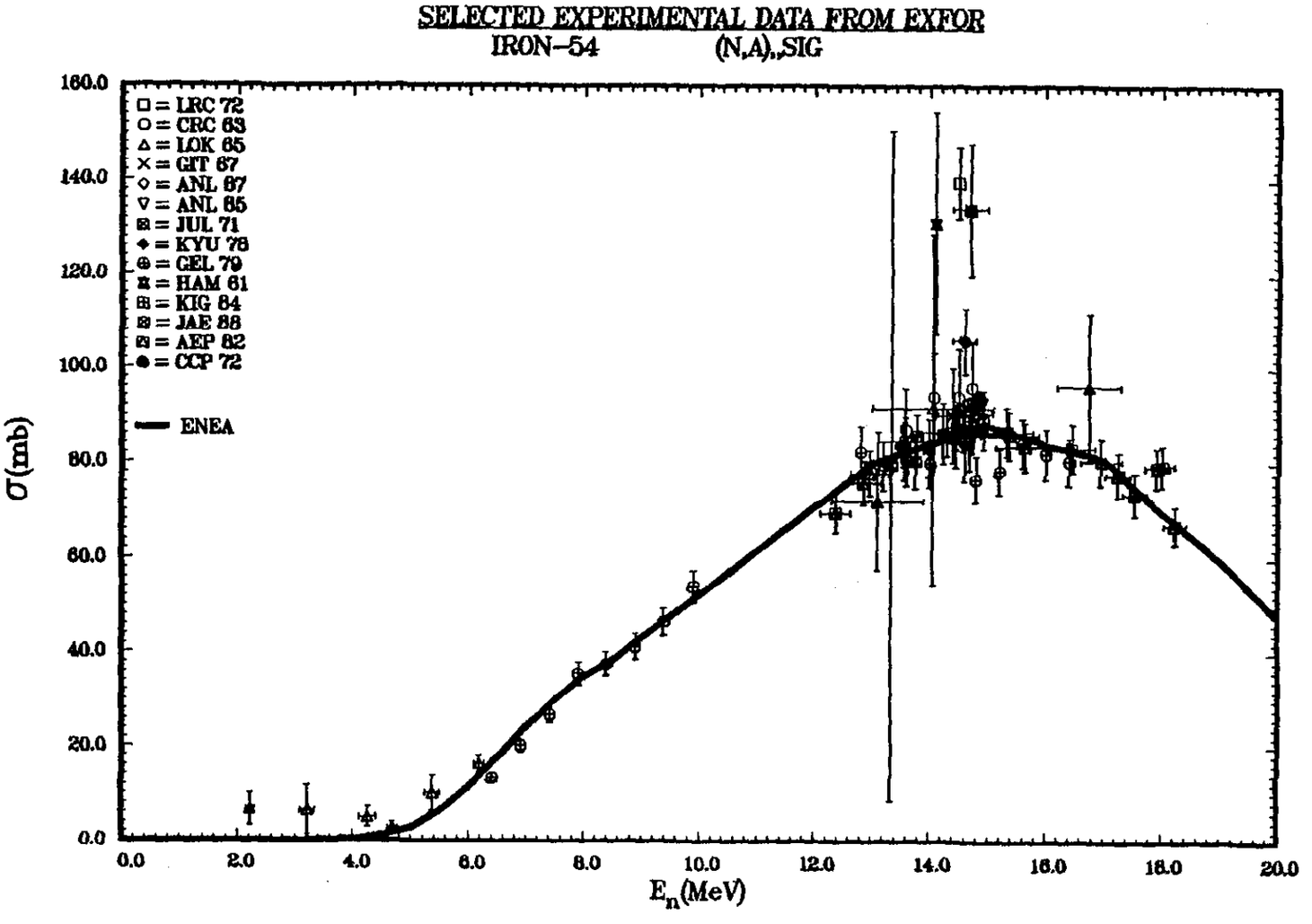

Fig. 12

SELECTED EXPERIMENTAL DATA FROM EXFOR
IRON-56 (N,TOT),,SIG

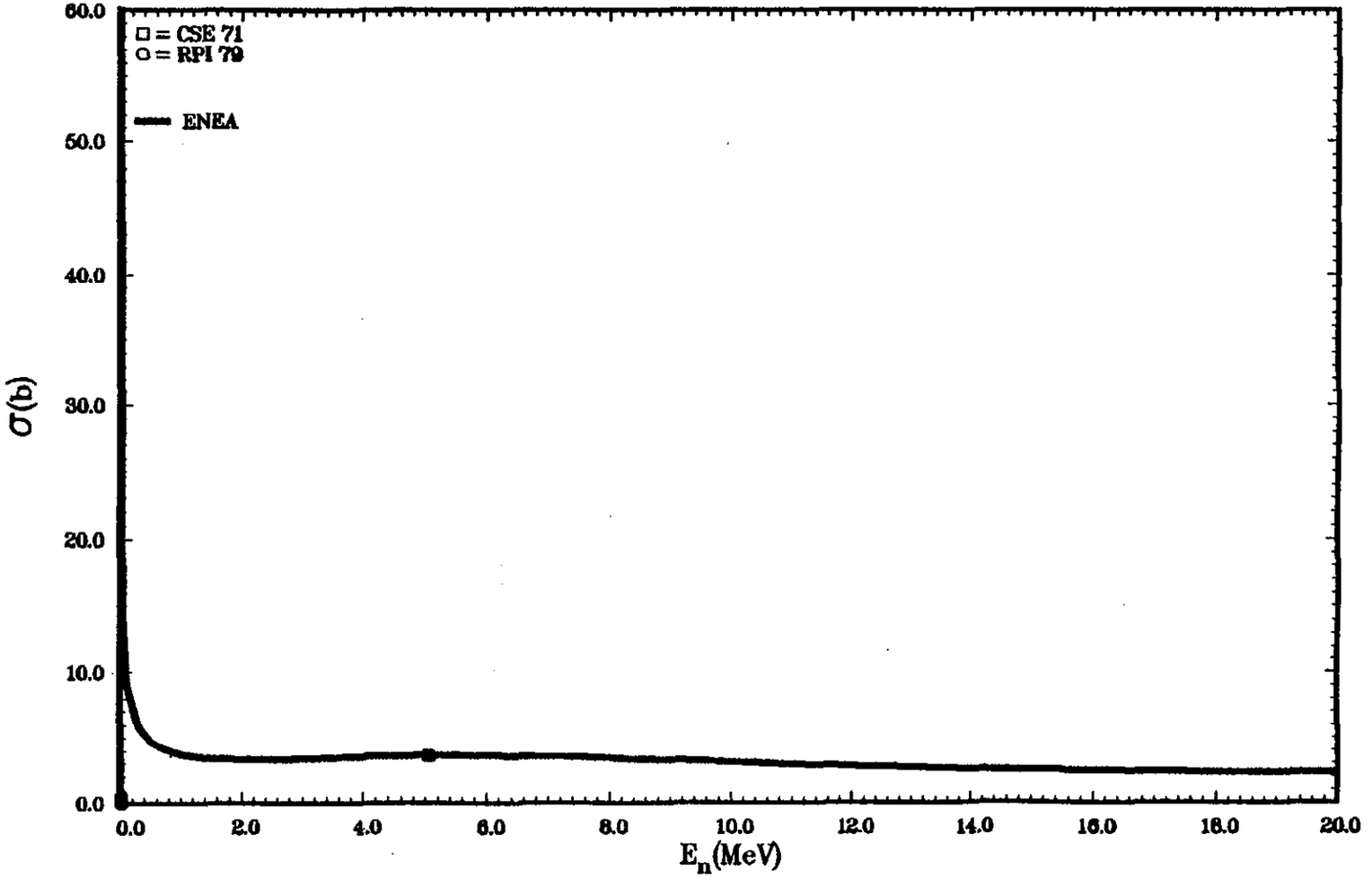

Fig. 13

SELECTED EXPERIMENTAL DATA FROM EXFOR
IRON-56 (N,EL),,SIG

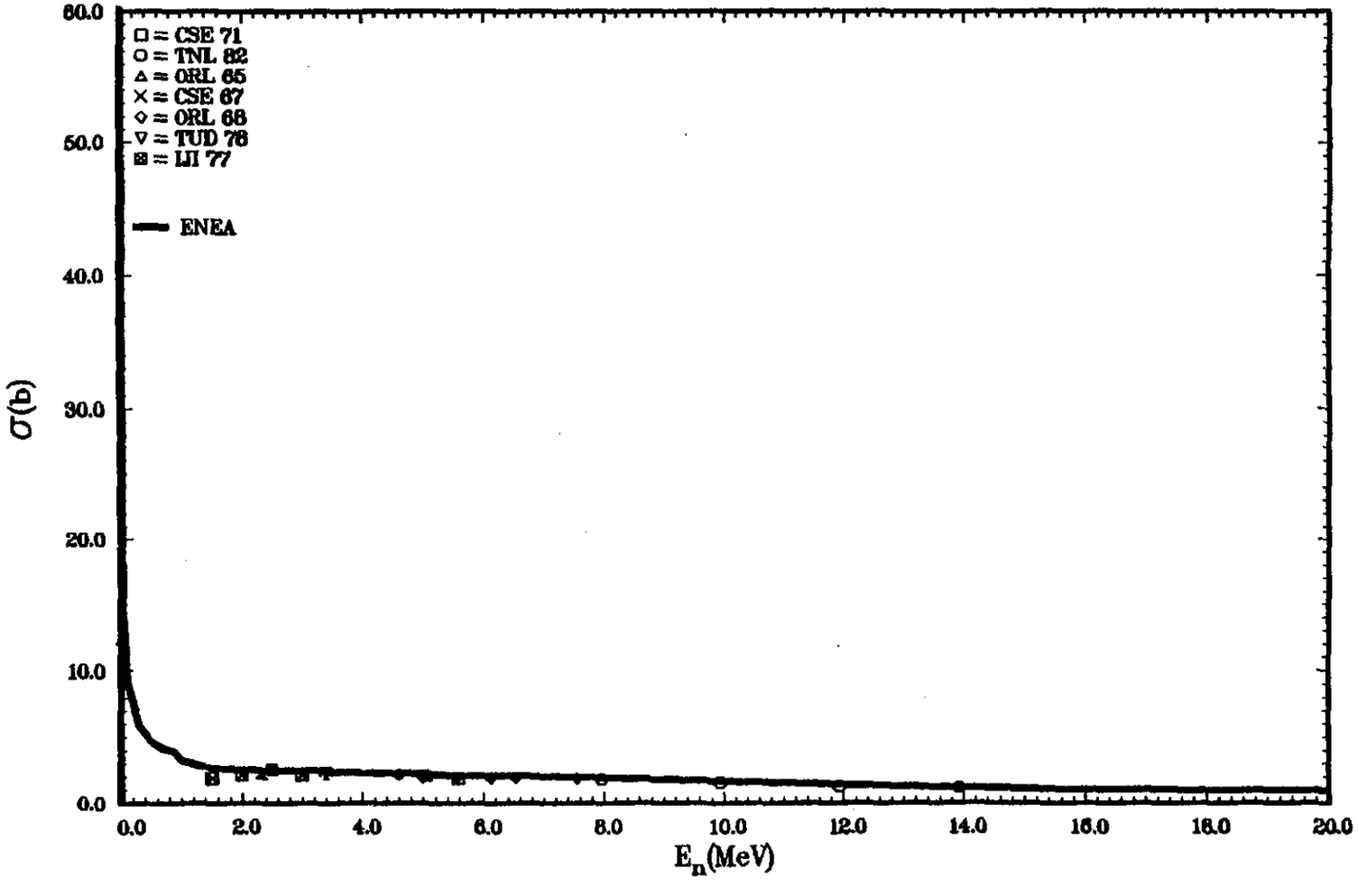

Fig. 14

1412049

SELECTED EXPERIMENTAL DATA FROM EXFOR
IRON-56 (N,P),,SIG

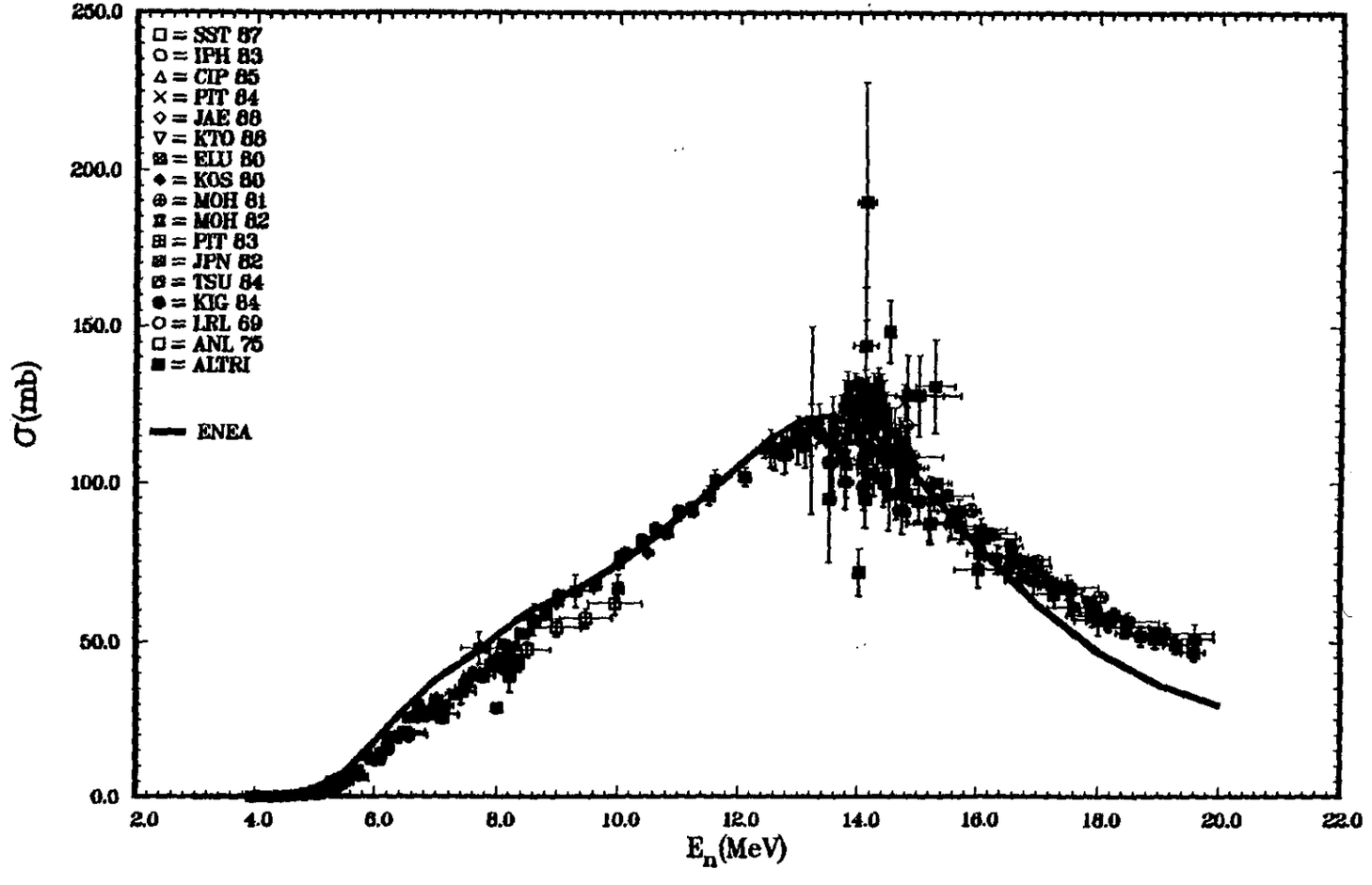

Fig. 15

14120050

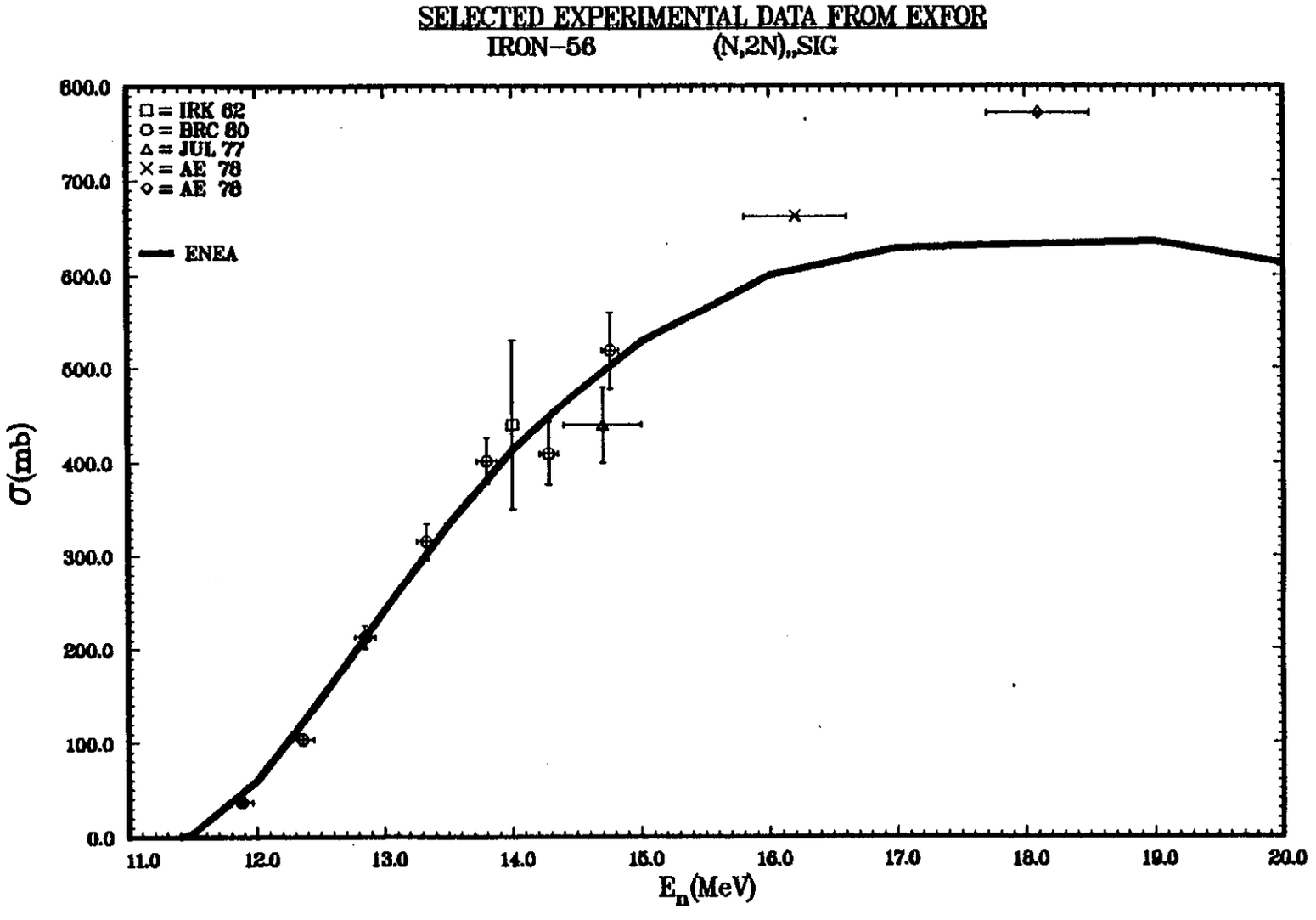

Fig. 16

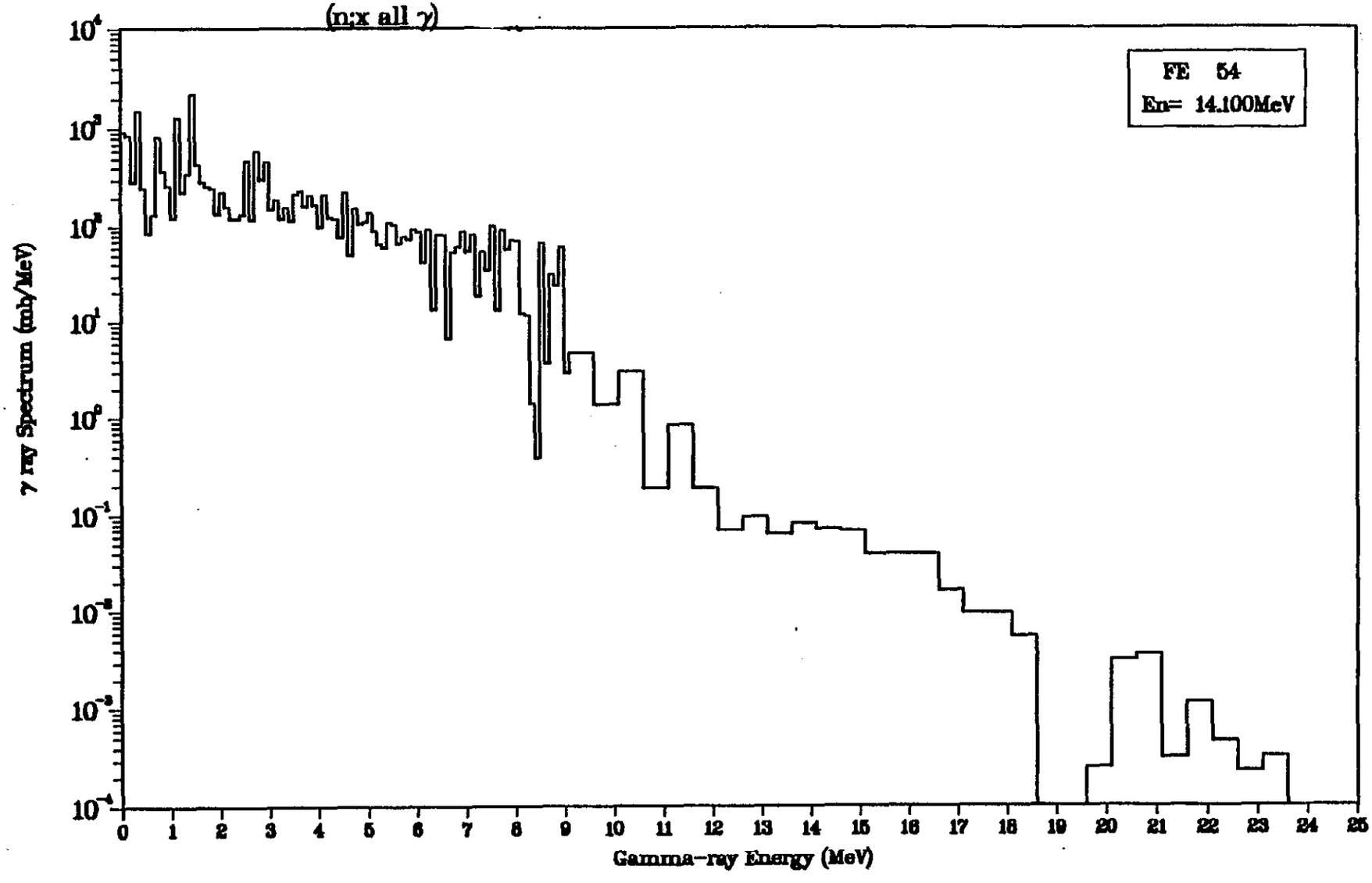

Fig. 17

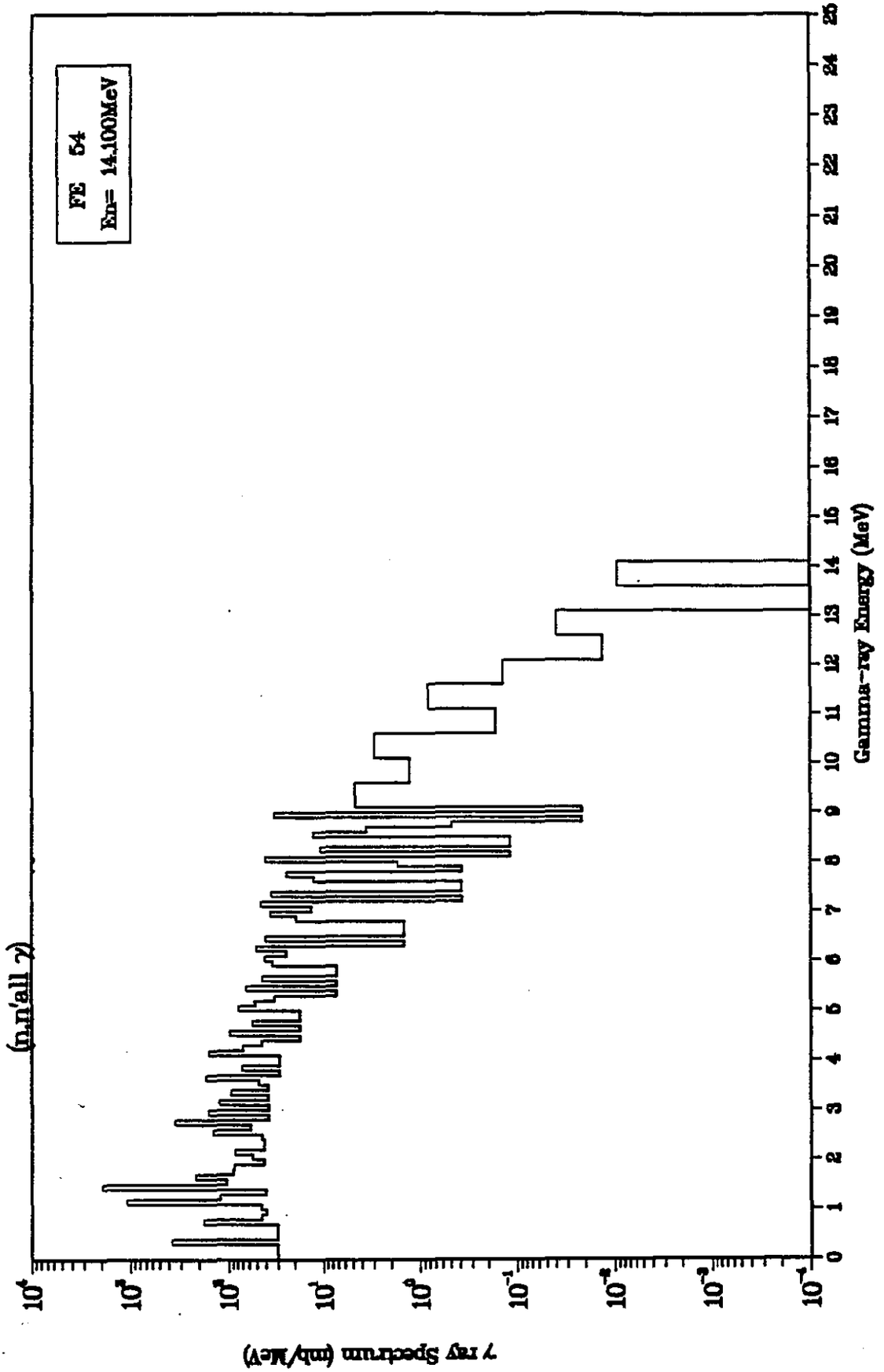

Fig. 18

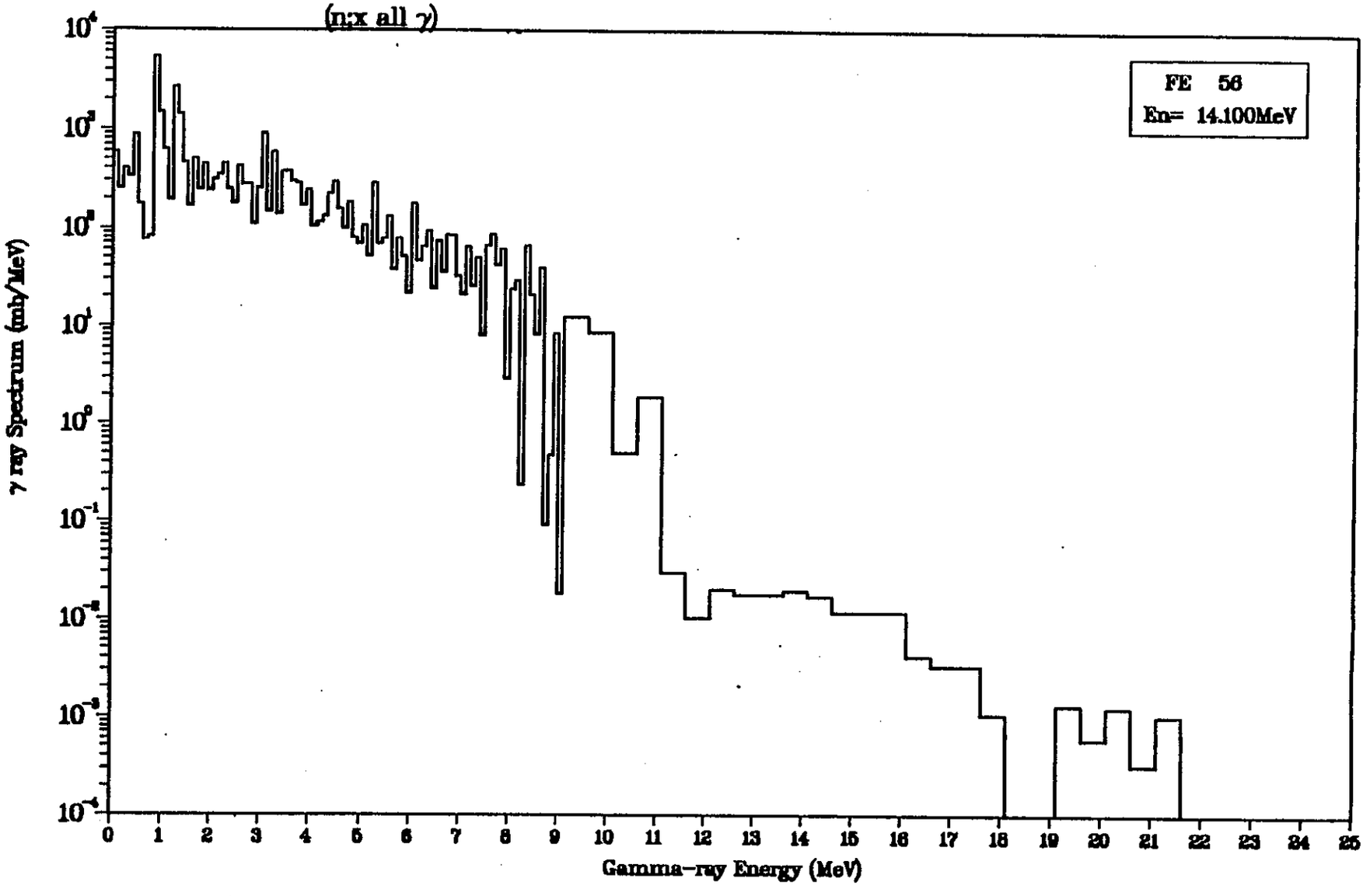

Fig. 19

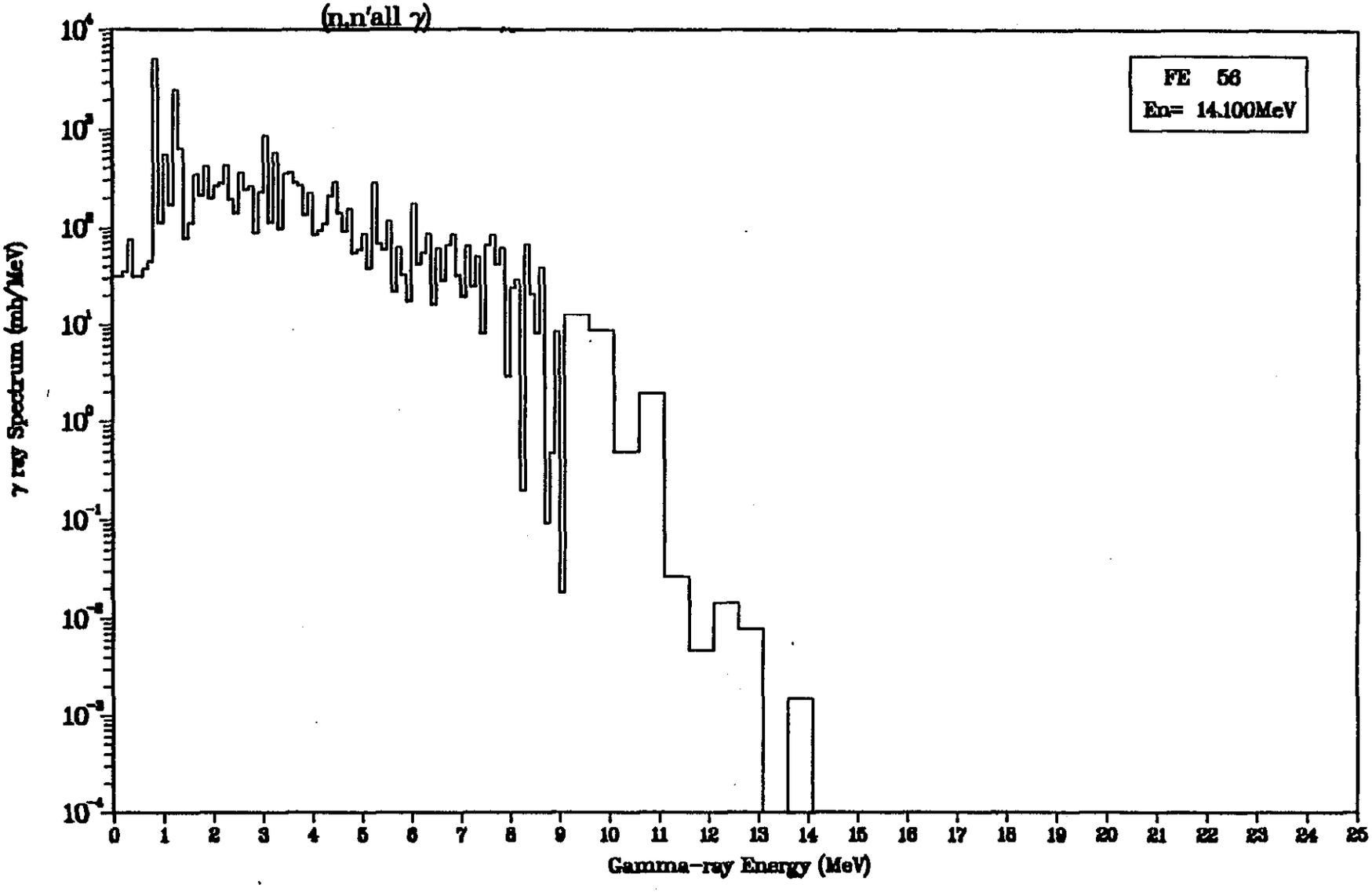

Fig. 20

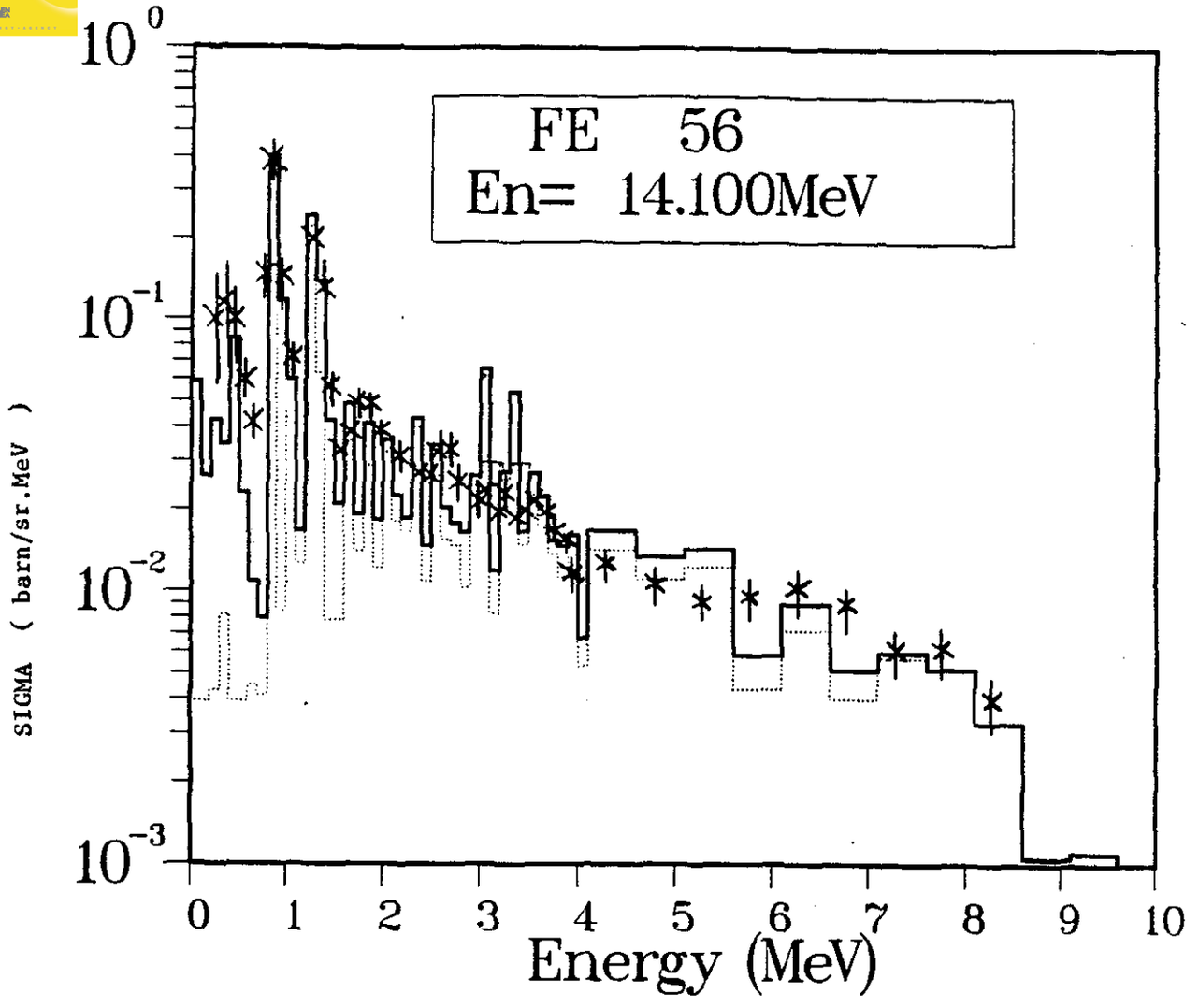

Fig. 21

Gamma-ray emission spectrum from $^{56}Fe(n,x\gamma)$ reactions at $\vartheta = 90°$ for 14.1 MeV incident neutrons. Experimental data are taken from : D.M.Drake, E.D.Arthur and M.G.Silbert, Nucl.Sci. Eng. 65, 49 (1978). Solid line : present calculations for total gamma-ray emission spectrum, namely $(n,n'\gamma)$, (n,γ), $(n,2n\gamma)$, $(n,p\gamma)$, $(n,np\gamma)$ and $(n,\alpha\gamma)$. Dotted line : present calculations for $(n,n'\gamma)$ channel only.

Fig. 22

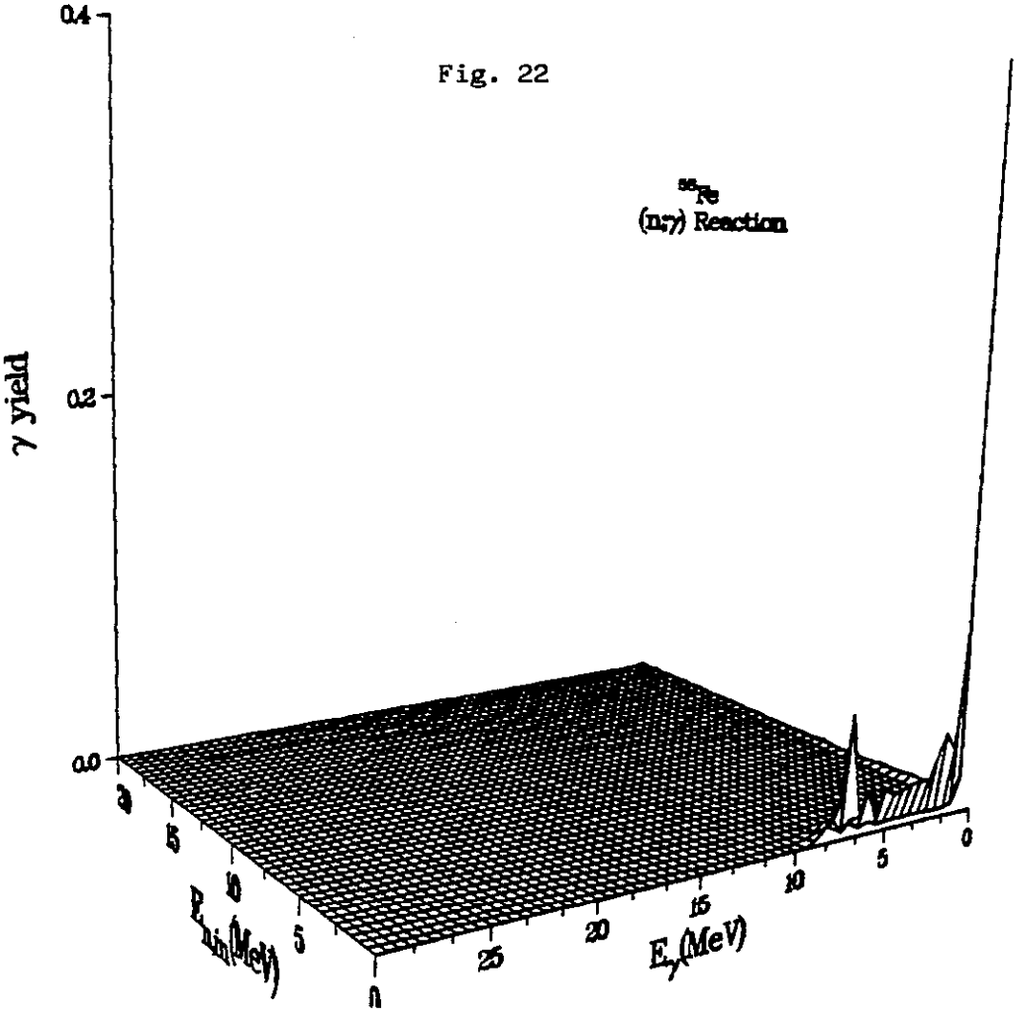

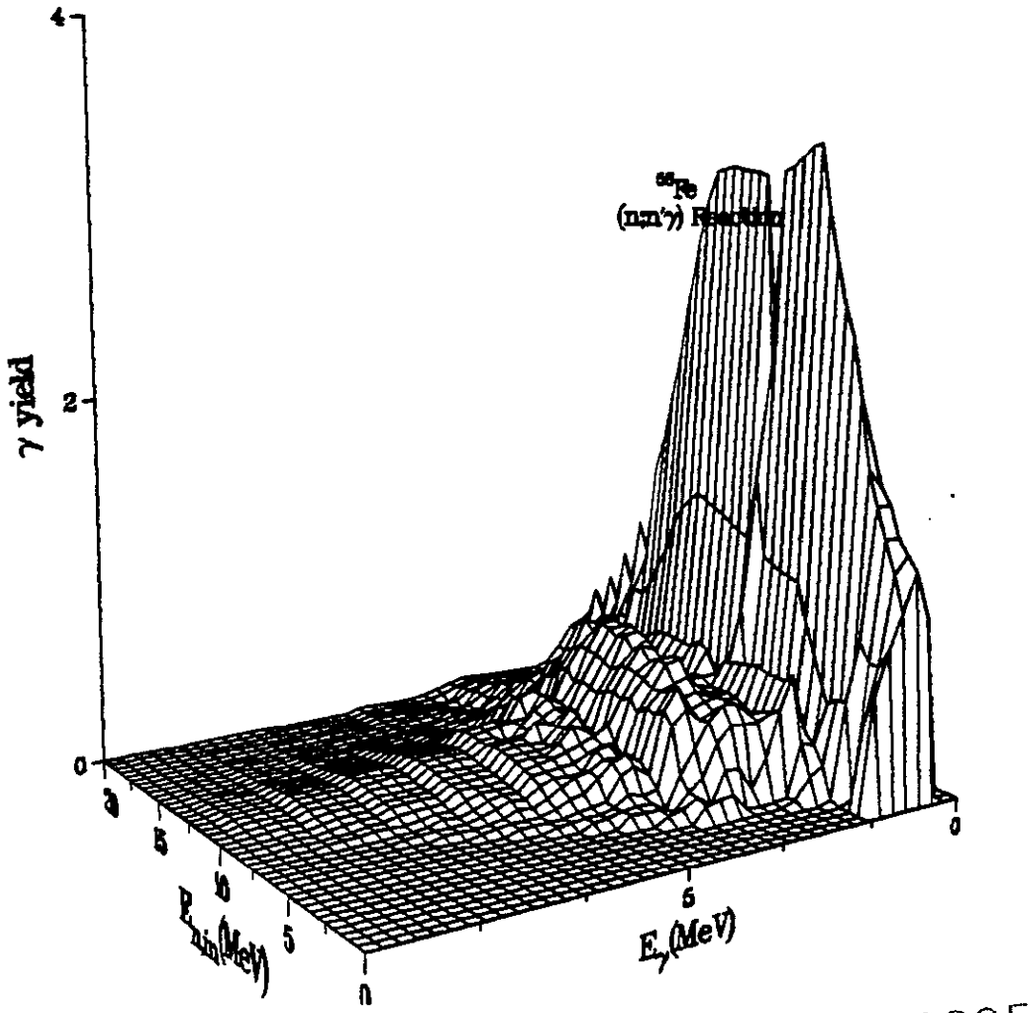

Fig. 23

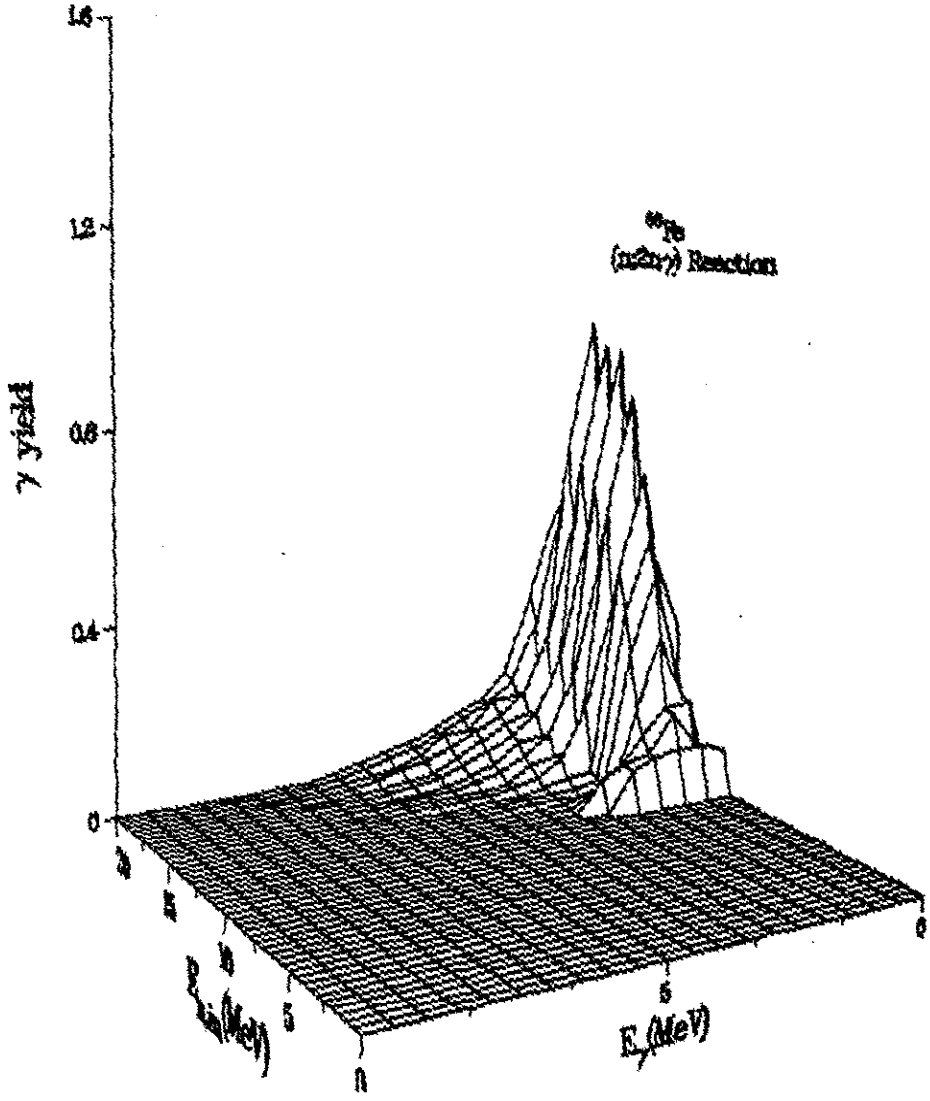

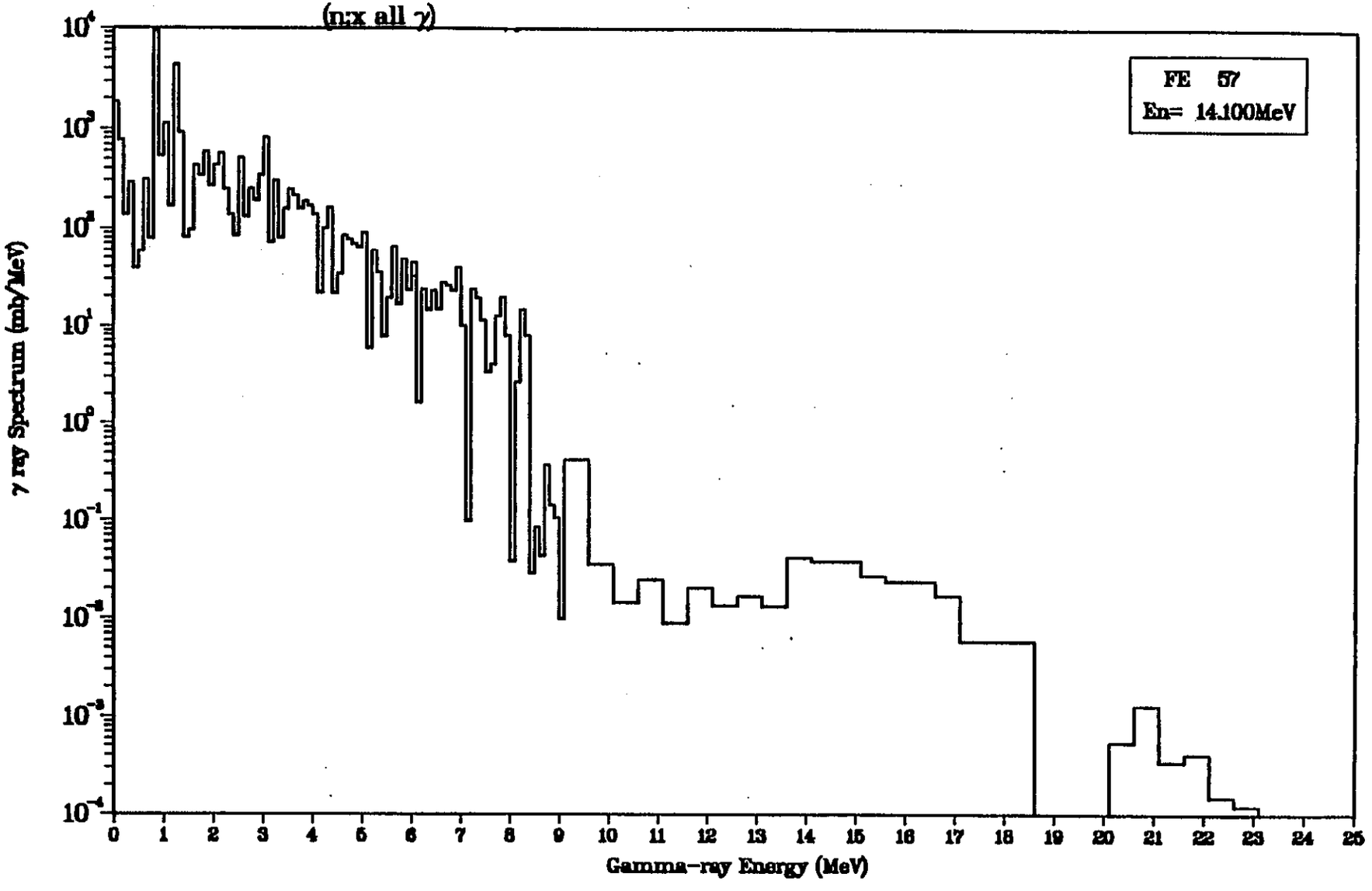

Fig. 24

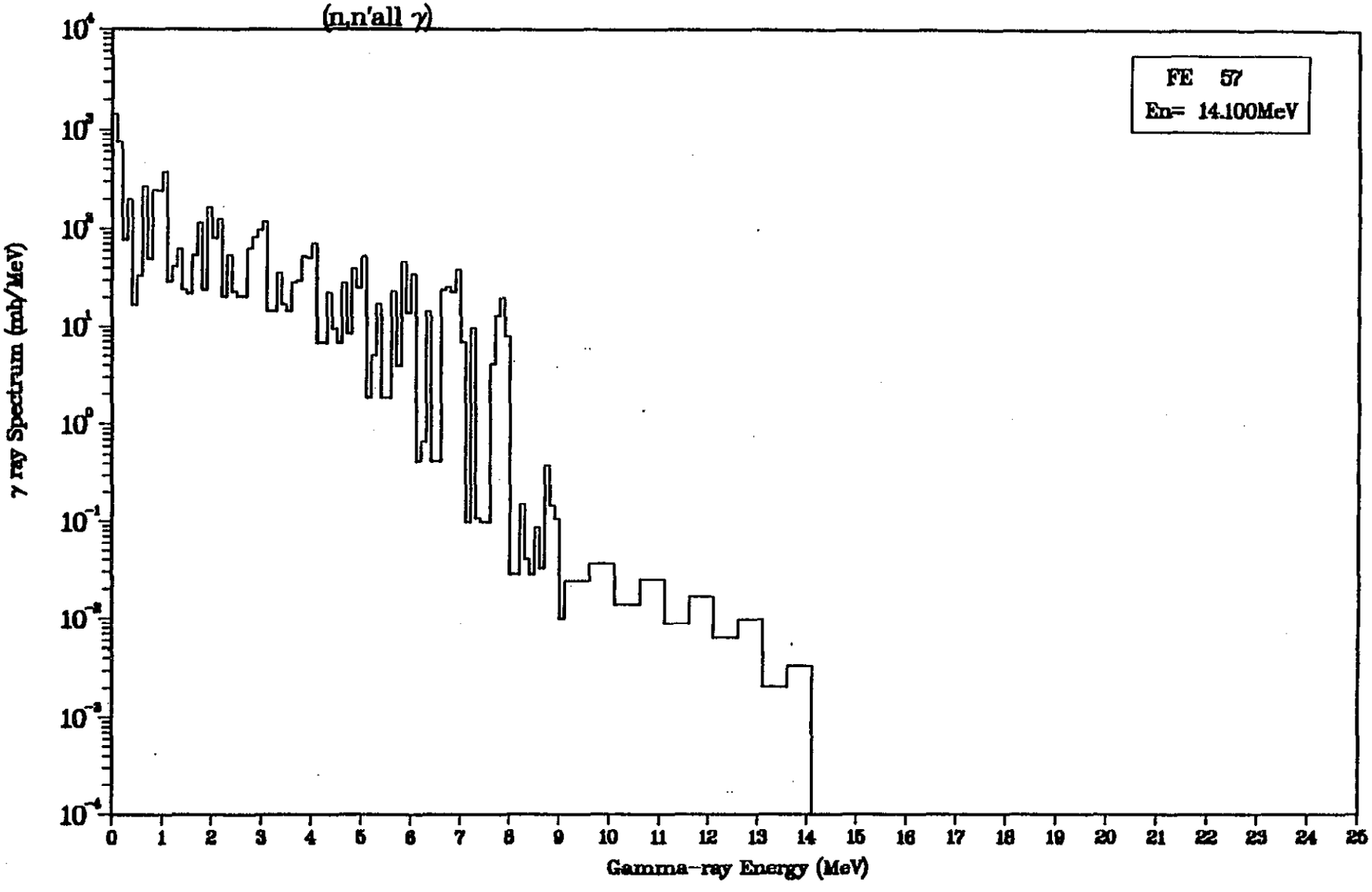

Fig. 25